Multiple Coordination Modes of a New Ditopic Bis(pyrazolyl)methane Ligand

Journal:	*Dalton Transactions*
Manuscript ID	DT-ART-10-2018-003992.R1
Article Type:	Paper
Date Submitted by the Author:	13-Nov-2018
Complete List of Authors:	Coulton, John; Eastern Illinois University, Chemistry and Biochemistry Smith, Aramis; Eastern Illinois University, Chemistry and Biochemistry Wheeler, Kraig; Whitworth University, Chemistry Semeniuc, Radu; Eastern Illinois University, Chemistry and Biochemistry

Journal Name

ARTICLE

Multiple Coordination Modes of a New Ditopic Bis(pyrazolyl)methane-Based Ligand

Received 00th January 20xx,
Accepted 00th January 20xx

DOI: 10.1039/x0xx00000x

www.rsc.org/

John B. Coulton,[a] Aramis C. Smith,[a] Kraig A. Wheeler,[b] and Radu F. Semeniuc[a]*

A new ditopic ligand, N-(2,2-bis(pyrazolyl)ethyl)-2,2-bis(pyrazolyl)acetamide ($(pz)_2CH$-C(O)-NH-CH_2-$CH(pz)_2$, L4Pz, pz = pyrazolyl ring), comprising of two bis(pyrazolyl)methane donor groups linked *via* an amide bridge, has been prepared from the reaction of $HOOCCH(pz)_2$ and $H_2NCH_2CH(pz)_2$. The ligand coordinates to various metallic salts (*i.e.* AgO_3SCF_3, $PdCl_2$, $Re(CO)_5Br$, and $Fe(BF_4)_2$), in either a κ^2-μ-κ^2 or a κ^3-μ-κ^2 fashion, depending on the coordination preferences of the metallic center. These compounds were characterized by NMR, UV-Vis and IR spectroscopy, and in solid state by single crystal X-ray diffraction. In the case of silver(I), a mono-dimensional coordination polymer was obtained, while the others were found to be discrete complexes. The synthesis and characterization of a heterobimetallic complex is also described. In solid state, all compounds are associated into supramolecular architectures *via* hydrogen bonding and pyrazolyl embrace interactions.

Introduction

Ever since they were introduced by Trofimenko in 1970,[1] bis- and tris(pyrazolyl)methane ligands have become major players in the field of coordination and supramolecular chemistry, catalysis, materials chemistry, and bioinorganic chemistry.[2] One important feature offered by the bis(pyrazolyl)methane donor set (-$C(pz)_2$, pz = pyrazolyl ring) is the possibility of backbone functionalization of the methylene carbon, thus providing access to more intricate ligand systems. Within this regard, two divergent directions have been pursued. The first approach is based on attaching a third donor group to the backbone of the bis(pyrazolyl)methane moiety to obtain the so called heteroscorpionate ligands, in which the coordination mode of the original donor set is changed from bidentate to tridentate. The second methodology consists of linking two or more bis(pyrazolyl)methane groups into one molecule, thus generating multitopic bidentate ligands that can support mono- and polymetallic species.

Some of the heteroscorpionates built on the bis(pyrazolyl)-methane scaffold are depicted in Chart 1. Pyridine and pyridine-like moieties have been used as the third donor group (compounds of type **A**),[3] and the metal complexes of these ligands have found applications in biomimetic catalysis[3a-c] or ethylene polymerization and oligomerization.[3d] Changing the position of the N atom within the pyridine ring (compounds **B**) provided access to a large variety of coordination networks and supramolecular frameworks.[4] Metal complexes having various catalytic activities were obtained by attaching a phenol onto the backbone of methylene group (compounds **C**).[5] Switching from phenol to a thioether group (compounds **D**) led to the formation of either porous molecular crystals or robust Ag(I) and Cu(I) coordination polymers.[6] Bis(pyrazolyl)ethanamine (**E**)[7] and its derivatives (**F**),[7,8] represent another class of versatile hetero-scorpionates, their metal complexes finding applications in supramolecular chemistry,[7a] or being investigated as imaging agents,[8a] or as novel photoactivatable CO-releasing molecules.[8c] Phosphorus-based groups were also used to in the synthesis of heteroscorpionates, as exemplified in Chart 1 by compounds **G** and **H**.[9,10] Their corresponding metal complexes were found to be active in ring-opening polymerization reactions.

Perhaps one of the most known and most important hetero-scorpionate ligand is the bis(pyrazolyl)acetic acid (Chart 1, compound **I**).[11] This compound, in its deprotonated form, acts as a tripodal ligand, and it can be further functionalized at the -C(O)OH end, to afford compounds of type **J**,[12] **K**,[13] and **L**.[14] While the ester ligand **J** was used to build dendritic architectures,[12b] the aluminum complexes of the acetamidate and thioacetamidate heteroscorpionates **K** were used to investigate ring-opening polymerization reactions.[13d,f] Zinc complexes of these ligands were probed as anticancer agents,[13b] while some copper-based compounds showed biological activity.[13c,e] The amidinate-based ligands **L**, in combination with magnesium and zinc centers, showed promise as selective ring-opening polymerization catalysts.[14]

On another hand, by grafting two -$C(pz)_2$ units onto a rigid central arene ring (Chart 2), several research groups produced ligands of the type **M**, **N**, and **O**. For example, Reger *et al.* prepared the *m*-bis[bis(1-pyrazolyl)methyl]benzene ligands (**M**) and observed the formation of bimetallic complexes of Mn(II),

---

[a] *Department of Chemistry and Biochemistry, Eastern Illinois University, Charleston, Illinois, 61920, United States.*

[b] *Department of Chemistry, Whitworth University, Spokane, Washington, 99251, United States.*

† Electronic Supplementary Information (ESI) available: Spectral characterization of all compounds and single crystal X-ray diffraction data. CCDC 1870002-1870006. See DOI: 10.1039/x0xx00000x

Fe(II), Co(II), Ni(II), Cu(II), Zn(II), and Cd(II), all having essentially the same metallacyclic structures containing a linear M-bridge-M core, (bridge = F$^-$, OH$^-$, CN$^-$, and N$_3^-$).[15] In the case of paramagnetic species, antiferromagnetic superexchange interactions were observed, with the magnitude of the coupling increasing along the series from left to right across the periodic table.[15d] The *p*-bis[bis(1-pyrazolyl)methyl]benzene ligand (**N**) produce either coordination polymers or discrete compounds, depending on the metallic center,[16] while the ligands based on the tetra(pyrazolyl)lutidine scaffold (compounds **O**) have been found to have different coordination behavior of the pyridine moiety: either not involved in coordination to the metal center in the case of Ag(I), or coordinated when the metal was Fe(II). In the latter case, substitution of the H atoms of the pyrazolyl ring with methyl groups led to changes in the ligand field strength.[17]

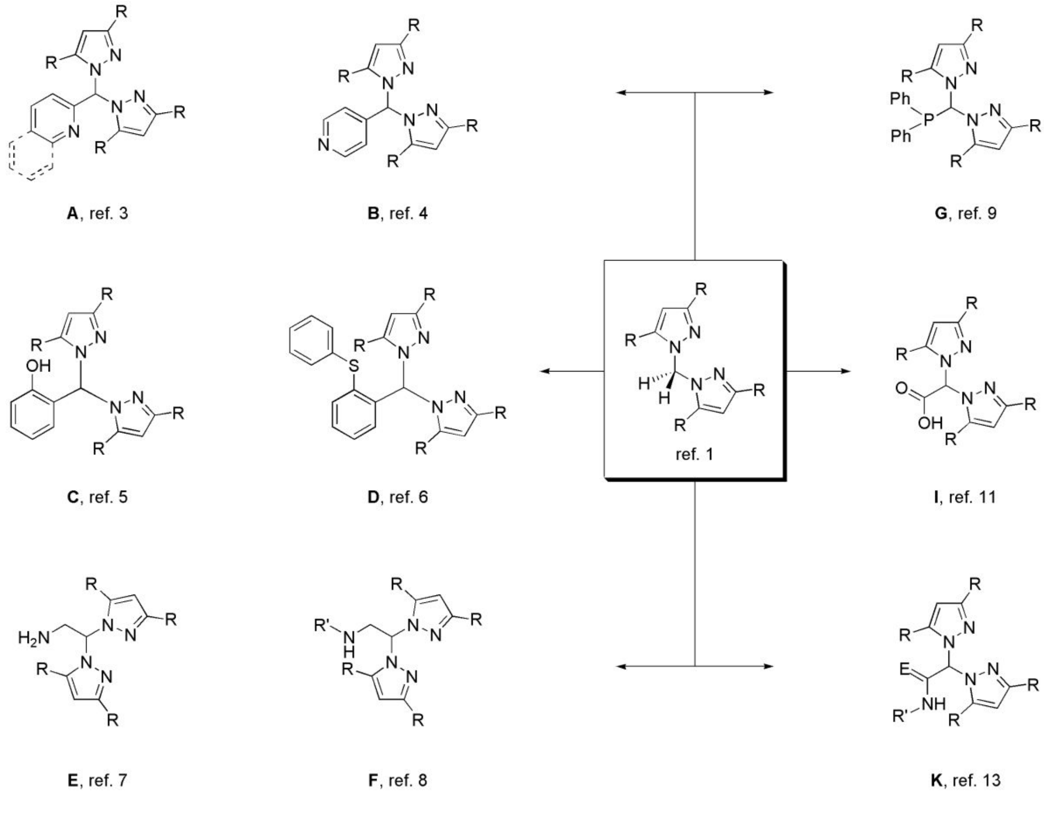

R = H, Me, i-Pr, t-Bu; Y = O or NAr; E = O or S; R' = various alphatic or aromatic groups

Chart 1. Heteroscorpionates based on backbone modification of the bis(pyrazolyl)methane ligand.

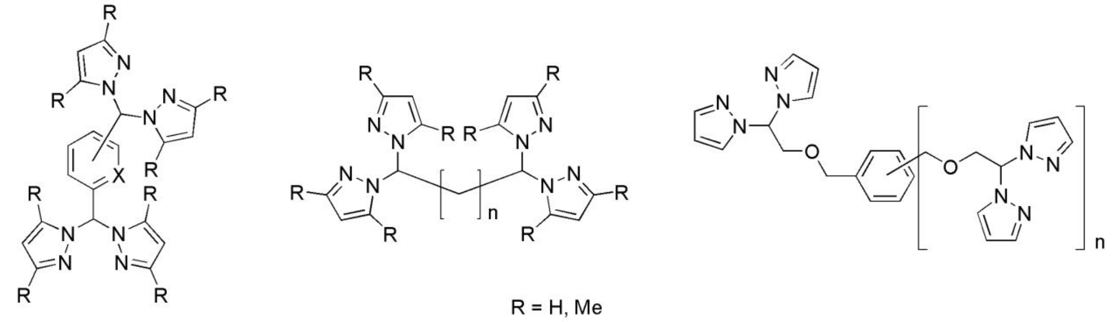

M, X = CH meta linked; ref. 15
N, X = CH para linked; ref. 16
O, X = N meta linked; ref. 17

P, n = 1, 2, 3
ref. 18

Q, n = 2, 3, 4, 6
ref.19

Chart 2. Ligands based on linking two or more -C(pz)$_2$ donor groups in one molecule.

Flexible spacers have also been used to link two or more -C(pz)$_2$ units in one molecule, producing ligands of type **P**[18],and **Q**.[19] These ligands, when coordinated to metallic centers, showed a propensity to form unusual metallacycles, although in some instances the formation of coordination polymers was also observed.

While the above examples clearly demonstrate the importance of bis(pyrazolyl)methane-based ligands in various facets of chemistry, this field still remains ripe for further developments. As part of our ongoing research efforts in the design and synthesis of ligands that can support mono- and polymetallic complexes,[20] we have started a project focused on finding new ways of linking two bis(pyrazolyl)methane donor sets into a single molecule. Our goal was to unify the two divergent directions described above and design a series of ditopic, bridging bis(pyrazolyl)methane ligands also capable of acting as heteroscorpionates; in other words, we wanted to identify a spacer that would offer both coordination versatility and structural flexibility to the resulting ligands. The design is depicted in Chart 3: starting from the well-known bis(pyrazolyl)-acetic acid and bis(pyrazolyl)ethanamine derivatives, an entire family of ligands having various substitution patterns of the pyrazolyl rings can be prepared. The ligands consist of two bis(pyrazolyl)methane donor groups bridged by an amide linkage. The modular synthesis of these ligands offers the possibility to prepare unsubstituted (Chart 3a), partly substituted (Chart 3b and 3c) or fully substituted (Chart 3d) ligands, thus offering the possibility of fine-tuning the steric properties around the metal center in the resulting complexes of these ligands.

Toward this end, we describe here the synthesis of the first member of this series (see Chart 3a), bearing two unsubstituted bis(pyrazolyl)methane donor units connected *via* the rigid amide spacer. Also reported are the reactions of this ligand with Ag(I), Pd(II), Re(I), and Fe(II) metallic centers, to form either coordination polymers or discrete metal complexes; these compounds were characterized by NMR, UV-Vis and IR spectroscopy, and in solid state by single crystal X-ray diffraction. A structural comparison of the structures is also presented.

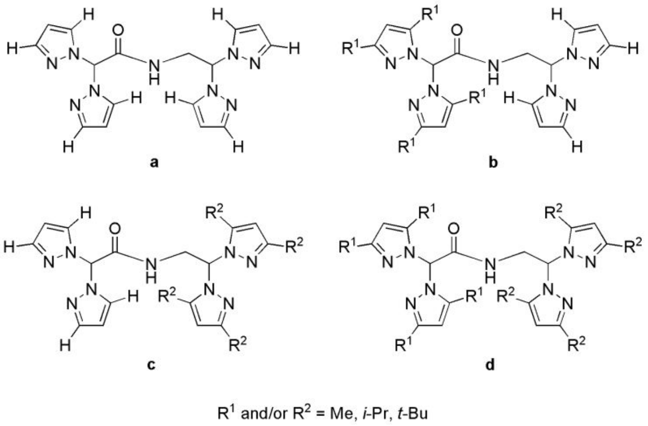

Chart 3. Amide bridged, ditopic bis(pyrazolyl)methane ligands.

Experimental

General Considerations

All operations were performed in ambient atmosphere. NMR spectra were recorded using a 400 MHz Bruker Avance FT-NMR Spectrometer. Infrared spectroscopy was performed on a Nicolet iS10 in a KBr matrix, and UV-Vis spectroscopic investigations were carried on a Cary 100 Agilent Spectrophotometer. Bis(pyrazolyl)acetic acid[19a] and bis(pyrazolyl)ethanamine $H_2N\text{-}CH_2\text{-}CH(pz)_2$[7a] and were prepared as described in the literature. All solvents and other reagents used in the syntheses described below are commercially available and used as received, without further purification.

The X-ray data were collected at 100 K on a Bruker SMART APEXII CCD diffractometer equipped with Cu-Kα radiation. Intensities were collected using phi and omega scans and were corrected for Lorentz polarization and absorption effects. The *X-SEED* software platform,[21] equipped with *SHELXS* and *SHELXL* modules on a PC computer,[22] was used for all structure solution and refinement calculations and molecular graphics. The structures were solved by direct methods and refined by anisotropic full-matrix least-squares for all non-hydrogen atoms. Crystal data, data collection and structure refinement details for all complexes are provided in Supporting Information.

Synthesis of N-(2,2-bis(pyrazolyl)ethyl)-2,2-bis(pyrazolyl)-acetamide ($(pz)_2CH\text{-}C(O)\text{-}NH\text{-}CH_2\text{-}CH(pz)_2$, L4Pz)

Method I: A 250 mL round bottom flask was charged with a stirring bar, THF (100 mL), and bis(pyrazolyl)acetic acid (3.844 g, 0.02 mol). To the resulting solution, dicyclohexylcarbodiimide (2.476 g, 0.012 mol) was added as a solid, and the mixture was stirred at room temperature. After 2 hours, a solution of bis(pyrazolyl)ethanamine (1.772 g, 0.01 mol) in 50 mL THF was added, and the mixture was stirred overnight. The formed urea was filtered off, and the solvent was removed under vacuum. The resulting oil was taken in dichloromethane (5 mL) and triturated with diethyl ether. The resulting white precipitate was isolated by vacuum filtration, washed with ether (3 x 25 mL) and dried in air. Yield 2.785 g (79 %). **Method II:** A 100 mL round bottom flask was charged with a stirring bar and pyridine (15 mL). Bis(pyrazolyl)acetic acid (0.961 g, 0.005 mol) was added portion wise, and the mixture was stirred with gentle heating until a clear solution was obtained. To this solution, solid bis(pyrazolyl)ethanamine (0.886 g, 0.005 mol) was added portion wise, and the resulting solution was heated for 15 minutes at 75 °C. At this point, triphenyl phosphite (1.565 mL, 0.006 mol, 1.2 equivalents) was added in one portion and the solution was heated under reflux overnight. After cooling to room temperature and removal of the volatiles, the resulting oil was taken in chloroform (200 mL). The organic phase was washed with diluted NH_4Cl solution (3 x 250 mL) and brine (3 x 250 mL), and then dried over anhydrous sodium sulfate. Removal of the solvent and trituration with diethyl ether produced the desired compound as a white powder (1.458 g, 83 %). ^{1}H-NMR (400 MHz, $CDCl_3$): δ = 7.68 (t, br, 1H, C(O)N*H*), 7.66-7.52 (m, 8H, 3,5-*H*pz), 6.92 (s, 1H, C*H*), 6.67 (t, J = 6.84 Hz, 1H, -C*H*-CH_2), 6.29-6.27 (m, 4H, 4-*H*pz), 4.41 (t, J = 6.48 Hz, 2H, -CH-CH_2). ^{13}C-NMR ($CDCl_3$): δ 164.39 (*C*(O)NH), 141.48 (*C*pz), 140.64 (*C*pz), 130.22 (*C*pz), 129.18 (*C*pz), 107.22 (*C*pz), 106.94 (*C*pz), 75.49 (*C*H_2), 72.32 (*C*H_2), 42.29 (*C*H). IR (KBr pellet, $\tilde{\nu}$ / cm^{-1}): 3238 (m), 3122 (m), 3071 (m), 1701 (s), 1569 (s), 1520 (s), 1443 (m), 1393 (s), 1296 (s), 1227 (m), 1093 (s), 1045 (s), 963 (m), 918 (m), 827 (m), 735 (s), 621 (s), 528 (w), 458 (w).

Synthesis of {[(L4Pz)Ag](O_3SCF_3)}$_n$, (1)

A 100 mL round bottom flask was charged with a stirring bar, THF (30 mL), **L4Pz** (0.176 g, 0.5 mmol) and AgO_3SCF_3 (0.128 g, 0.5 mmol). After 2 hrs. of stirring hexanes (50 mL) were added to the cloudy solution and the resulting precipitate was isolated by vacuum filtration, washed with hexanes and dried in air, to yield the desired compound as a white powder (0.227 g, 75 %). ^{1}H-NMR (400 MHz, acetone-d_6): δ = 8.21 (d, J = 2.56 Hz, 2H, 3,5-*H*pz), 8.06-8.05 (m, br, 3H, 2H, 3,5-*H*pz overlap with 1H, C(O)N*H*), 7.81-7.79 (m, 4H, 3,5-*H*pz), 7.77 (s, 1H, C*H*), 7.23 (t, J = 6.68 Hz, 1H, -C*H*-CH_2), 6.51-6.48 (m, 4H, 4-*H*pz), 4.53 (t, J = 6.36 Hz, 2H, -CH-CH_2). IR (KBr pellet, $\tilde{\nu}$ / cm^{-1}): 3243 (m), 3119 (m), 3078 (w), 2977 (w), 1697 (s), 1570 (m), 1519 (m), 1438 (m), 1394 (s), 1265 (s), 1167 (s), 1092 (s), 1037 (s), 998 (m), 969 (m), 917 (w), 762 (s), 709 (w), 644 (s), 520 (M), 459 (w).

Synthesis of $[(L4Pz)(PdCl_2)_2]$, (2)

A 250 mL round bottom flask was charged with a stirring bar, acetonitrile (100 mL), **L4Pz** (0.088 g, 0.25 mmol) and $(CH_3CN)_2PdCl_2$ (0.130 g, 0.5 mmol). After 24 hrs. of stirring, hexanes (50 mL) were added to the cloudy solution and stirred for one more hour. The resulting precipitate was isolated by vacuum filtration, washed with hexanes and dried in air, to yield the desired compound as an orange powder (0.124 g, 70 %). ^{1}H-NMR (400 MHz, acetonitrile-d_3): δ = 8.25-8.12 (m, 8H, 3,5-*H*pz), 7.71 (s, 1H, C*H*), 7.23 (t, br, 1H, C(O)N*H*), 7.12 (t, J = 6.61 Hz, 1H, -C*H*-CH_2), 6.58 (t, J = 2.4 Hz, 2H, 4-*H*pz), 6.49 (t, J = 2.1 Hz, 2H, 4-*H*pz), 4.63 (m, 2H, -CH-CH_2). IR (KBr pellet, $\tilde{\nu}$ / cm^{-1}): 3527 (m, br), 3122 (m), 2940 (w), 1709 (s), 1618 (m), 1519 (s), 1459 (s), 1414 (s), 1354 (w), 1295 (s), 1210 (m), 1104 (m), 1070 (s), 1000 (m), 907 (w), 854 (w), 736 (s), 712 (w), 613 (m), 566 (w), 458 (w).

Synthesis of $\{(L4Pz)[Re(CO)_3][Re(CO)_3Br]\}Br$, (3)

A 100 mL round bottom flask was charged with a stirring bar, toluene (75 mL), **L4Pz** (0.088 g, 0.25 mmol) and $Re(CO)_5Br$ (0.203 g, 0.5 mmol). The resulting mixture was heated under reflux overnight. After cooling to room temperature, the formed precipitate was filtered under vacuum, washed with diethyl ether and dried in air, to yield the desired compound as a yellow-orange powder (0.197 g, 75 %). ^{1}H-NMR (400 MHz, acetone-d_6, all br.): δ = 10.29 (1H, C(O)N*H*), 8.69 (3H, 2H, 3,5-*H*pz overlap with 1H, C*H*), 8.52 (2H, 3,5-*H*pz), 8.20 (2H, 3,5-*H*pz), 8.10 (2H, 3,5-*H*pz), 7.52 (1H, -C*H*-CH_2), 6.82 (2H, 4-*H*pz), 6.35 (2H, 4-*H*pz), 4.61 (2H, -CH-CH_2). IR (KBr pellet, $\tilde{\nu}$ / cm^{-1}): 3440 (m, br), 3241 (w), 3118 (w), 2956 (w), 2043 (s), 2028 (s), 1912 (s, br), 1648 (s), 1458 (w), 1411 (m), 1292 (m), 1244 (w), 1109 (w), 1068 (m), 995 (w), 765 (m), 651 (w), 610 (w), 532 (w), 495 (w).

Synthesis of $[(L4Pz)_2Fe](BF_4)_2$, (4)

A 100 mL round bottom flask was charged with a stirring bar, methanol (50 mL), **L4Pz** (0.176 g, 0.5 mmol) and $Fe(BF_4)\cdot 6\ H_2O$ (0.084 g, 0.25 mmol). After 2 hrs. of stirring, the cloudy solution was concentrated to 5 mL. The resulting precipitate was filtered under vacuum, washed with diethyl ether and dried in air, to yield the desired compound as a white powder (0.211 g, 91 %). IR (KBr pellet, $\tilde{\nu}$ / cm^{-1}): 3421 (m, br), 3330 (m), 3016 (w), 1659 (s), 1581 (w), 1519 (m), 1450 (m), 1405 (s), 1292 (s), 1237 (w), 1084 (s), 983 (m), 918 (w), 835 (w), 763 (s), 712 (w), 654 (w), 620 (w), 533 (w), 455 (w).

Synthesis of $[(L4Pz)_2FeAg](BF_4)_3$, (5)

A 100 mL round bottom flask was charged with a stirring bar, acetonitrile (50 mL), $\mathbf{[(L4Pz)_2Fe](BF_4)_2}$ (0.093 g, 0.1 mmol), and $AgBF_4$ (0.020 g, 0.1 mmol). After two hours of stirring and removal of the solvent under vacuum, the title compound was isolated as a white powder (0.103 g, 91%). IR (KBr pellet, $\tilde{\nu}$ / cm^{-1}): 3342 (m), 3128 (m), 3039 (w), 2947 (w), 1659 (s), 1560 (w), 1521 (m), 1448 (m), 1402 (s), 1295 (s), 1226 (w), 1204 (w), 1060 (s, br), 919 (w), 957 (w), 832 (w), 768 (s), 715 (w), 655 (w), 618 (m), 522 (m), 458 (m).

Results and Discussion

Ligand design and synthesis

In our design of a new ditopic bis(pyrazolyl)methane ligand we chose an amide moiety as a bridge between two bis(pyrazolyl)-methane groups for several reasons. First, the -NHC(O)- linkage is rigid and robust, but also versatile, as demonstrated by the protein architectures capable of performing complex tasks in biological systems. Second, the amide group has both hydrogen bond accepting and donating properties, thus providing the possibility of supramolecular association of the resulting metal complexes. Finally, this group can bind to metallic centers either *via* the oxygen atom in the case of neutral amides, or *via* the nitrogen atom in the case of deprotonated amides.[23] As such, within the new ligand N-(2,2-bis(pyrazolyl)ethyl)-2,2-bis-(pyrazolyl)acetamide ($(pz)_2CH\text{-}C(O)\text{-}NH\text{-}CH_2\text{-}CH(pz)_2$, **L4Pz**, see Figure 1), the bidentate (κ^2) bonding mode of the -$C(pz)_2$ donor set is encoded in each of the bis(pyrazolyl)methane moieties, thus offering **L4Pz** the possibility to act as a κ^2-μ-κ^2 ligand. In addition, the presence of the amide group offers additional possibilities of coordination to a metallic center, thus changing the "amide end" of the ligand from a bidentate to a tridentate (heteroscorpionate, tripodal, κ^3) coordinating group; consequently, the ligand can coordinate in a κ^3-μ-κ^2 fashion to two metallic centers.

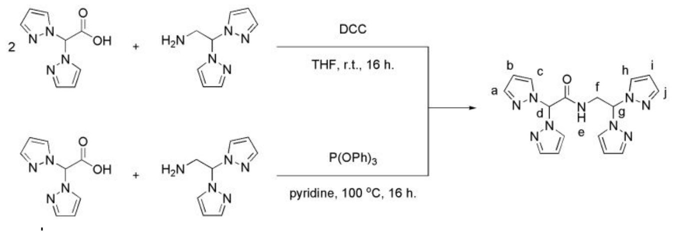

Scheme 1. Synthetic paths toward the **L4Pz** ligand; also given is the proton labeling scheme.

The ligand can be prepared on a multigram scale in good yields following two synthetic routes, see Scheme 1. The first involves the reaction of two equivalents of bis(pyrazolyl)acetic acid with one equivalent of bis(pyrazolyl)ethanamine, in the presence of dicyclohexylcarbodiimide (DCC),[24] and the second the reaction of the same components in a 1 : 1 ratio in the presence of triphenylphosphite.[25] While the work-up procedure is much simpler in the first case, the use of two equivalents of acid might appear as a waste of starting material. Regardless of the method used, the ligand is obtained in good yields as a white powder, soluble in most organic solvents (except diethylether and hexanes) and insoluble in water.

The ^{1}H- and ^{13}C-NMR spectra show the expected set of peaks for this ligand (see Figures S1 and S2 in the Supporting Information section). The amide proton (e in Scheme 1) appears at various ppm values, depending on the solvent. The C-H proton of the "amide end" of the ligand (d) appears as a singlet above 7 ppm, while the hydrogen atoms of the "amine end" (f and g) are easily identified above 4 and 6 ppm, respectively. The pyrazole hydrogen atoms show signals above 7 ppm (a, c, h, and j) and around 6 ppm (b and i). The ^{13}C-NMR spectrum shows the carbonyl peak at 164.39 ppm, the pyrazolyl peaks at 141.48/140.64, 130.22/129.18, and 107.22/106.94 ppm, respectively, and the aliphatic carbon atoms at 75.49, 72.32, and 42.29 ppm, respectively. The IR spectrum of the ligand recorded in a KBr matrix shows the characteristic amide stretching vibrations at 3122 cm^{-1} ($\tilde{\nu}_{NH}$) and 1701 cm^{-1} ($\tilde{\nu}_{CO}$), as well as pyrazolyl's C=N and N=N stretching vibrations at 1569 cm^{-1}.

Metal complexes syntheses and characterization

The reaction of **L4Pz** with Ag(O_3SCF_3), $(CH_3CN)_2PdCl_2$, Re(CO)$_5$Br, and Fe(BF_4)$_2$ produced the corresponding metal complexes described below. As a general synthetic method, the starting materials were dissolved in an appropriate solvent and mixed; upon stirring (either at room temperature or at reflux), the compounds precipitated out as powders in good yields. All complexes are light, air, and moisture stable, soluble in various organic solvents, but not in diethyl ether and hexanes. Their composition and structures have been established based on their analytical, spectral, and single-crystal X-ray diffraction data (*vide infra*). The crystal and refinement data are summarized in Table S1 in the Supporting Information, and essential structural parameters are presented separately with each complex. In two cases (*i.e.* the silver(I) and rhenium(I) complexes) the solvent molecules of crystallization were found to be severely disordered. After several attempts to model the disorder, the squeeze technique was used to account for and systematically remove diffraction data associated with these less well behaved species.

{[(L4Pz)Ag](O_3SCF_3)}$_n$, (1). The reaction of **L4Pz** with Ag(O_3SCF_3) in a 1 : 1 ratio in THF at room temperature produced a white precipitate that was isolated by vacuum filtration. The compound is soluble in methanol, acetone, acetonitrile, DMF, and DMSO, but not soluble in halogenated solvents.

Investigation of the ^{1}H-NMR spectrum of the complex in acetone-d$_6$ (Figure S3) revealed that the amide proton (e) maintained its chemical shift at 8.02 ppm, while the C-H proton (d) experienced a downfield shift of 0.56 ppm. These data suggest that not the amide proton, but rather the C-H proton (d) experiences a deshielding effect, presumably because of its involvement in hydrogen bonds either with the triflate counter-ion or the solvent. The IR spectrum of the complex (Figure S3) revealed practically no shift for the C=O stretching vibration (1694 cm^{-1}), a strong indication that the amide group is not involved in coordination to the Ag(I) center.

To further probe the structure of this compound, single crystals of the complex, suitable for X-ray diffraction studies, were grown over the course of a few days by diethyl ether vapor diffusion into an acetone solution of the complex. Crystallographic studies revealed that the asymmetric unit contains one ligand molecule, a Ag(I) cation and a triflate counter-ion. The coordination environment around the Ag$^+$ cation is depicted in Figure 2a, and consists in a distorted tetrahedral geometry, with the distortion caused by the "bite" angle of the two bis(pyrazolyl)methane donors. The degree of distortion from an ideal geometry in the case of four-coordinated metallic centers can be described by the angular parameter τ_4. This parameter can be calculated by subtracting the sum of the two largest angles from 360, then dividing the result by 141.[26] The obtained values would range from 1.00 for a perfect tetrahedral geometry to 0.00 for a perfect square planar geometry. In this case, the τ_4 value is 0.74, clearly indicative of a distorted tetrahedral geometry, rather than a distorted square planar environment.

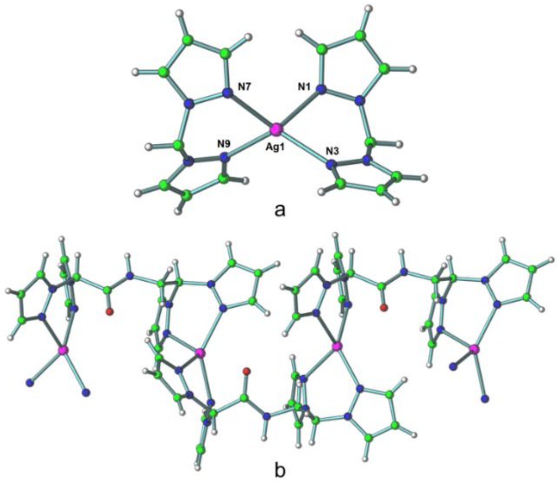

Figure 2. a) The coordination environment around Ag(I) and b) the structure of the cationic strand in **1**; selected bond and angles (Å and °): Ag(1)-N(1) = 2.372; Ag(1)-N(3) = 2.259; Ag(1)-N(7) = 2.287; Ag(1)-N(9) = 2.303; N(1)-Ag(1)-N(7) = 112.06; N(3)-Ag(1)-N(9) = 122.26; N(1)-Ag(1)-N(9) = 116.29; N(3)-Ag(1)-N(7) = 138.91; color code: carbon–green, hydrogen–gray, oxygen–red, nitrogen–blue, silver–purple.

The overall structure consists of a mono-dimensional coordination polymer built up by a κ^2-μ-κ^2 coordination mode of **L4Pz** to the Ag(I) center, see Figure 2b. The silver center is coordinated by two ligand molecules: one binds to the metal with the “amide end” while the other with the “amine end”, leading to a zipper-like shape of the 1D strand. Figure 3 depicts how these strands are organized into a bi-dimensional sheet-like supramolecular structure by C-H···O hydrogen bonds. As shown in Figure 3c by the blue dotted lines, each $F_3CSO_3^-$ anion bridges two adjacent strands, the C-H···O interaction parameters being 2.204 Å for the C(10)-H(10)···O(3) distance, 3.152 Å for the C(10)···O(3) distance, and 157.90° for the C(10)-H(10)-O(3) angle. While not very close contacts (the sum of van der Waals radii of oxygen and hydrogen atoms is 2.68 Å),[27] the C(10)-H(10)-O(3) angle is well above 130°; for this type of weak interactions (*i.e.* weak C-H···O hydrogen bonds), angles above this value indicate a substantial interaction between the O and H atoms, even in cases where the distances are close to the sum of van der Waals radii.[28]

The data presented above suggest that the solution structure of compound **1** is similar to the one observed in solid state. Looking at the ^{1}H-NMR spectra of the ligand and its Ag(I) complex, the amide proton experiences no shift upon complexation of the ligand to the metal center, clearly indicating its non-involvement in supramolecular interactions, while the downfield shift of the C-H proton (d) by 0.56 ppm strongly suggests its participation in a hydrogen bond, both facts confirmed by the solid state structure of **1**. Further, the IR data collected on the bulk powder is also in agreement with the results of our crystallographic studies, both showing the fact that the O atom from the amide group is not involved in the coordination of **L4Pz** to the silver(I) center.

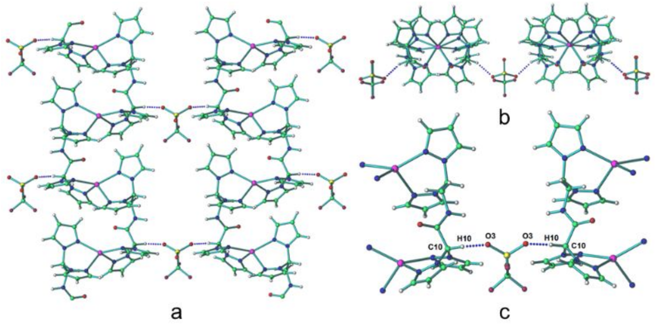

Figure 3. The supramolecular structure of **1**: a) perpendicular and b) parallel view of the 2D sheet-like structure; c) details of the C-H···O hydrogen bonds.

[(L4Pz)(PdCl$_2$)$_2$], (2). The reaction of **L4Pz** with $(CH_3CN)_2PdCl_2$ in a 1 : 2 ratio in acetonitrile, followed by addition of a small volume of hexanes, produced a light orange precipitate that was isolated by vacuum filtration. The compound is soluble in DMSO and DMF, and slightly soluble in acetonitrile; other solvents failed to dissolve this compound.

The ^{1}H-NMR spectrum of **2** in acetonitrile (Figure S4) shows an upfield shift for the N-H proton (e) ($\Delta\delta$ = 0.27 ppm), suggesting a shielding effect, and a downfield shift for the C-H proton (d) ($\Delta\delta$ = 0.68 ppm), indicative of its involvement in hydrogen bonding interactions. As with **1**, the IR spectrum of the palladium complex (Figure S4) revealed virtually no shift for the C=O stretching vibration (1708 cm^{-1}), suggesting that the amide oxygen atom is not involved in coordination to the Pd(II) center.

Single crystals of **2** were grown by slow evaporation of a DMSO solution of the complex and subjected to X-ray diffraction studies. The asymmetric unit consists of a [(**L4Pz**)(PdCl$_2$)$_2$] molecule and a DMSO molecule of crystallization; the molecular structure of the complex is presented in Figure 4a. **L4Pz** acts as a κ^2-μ-κ^2 ligand, with each end of the ligand chelating one PdCl$_2$ center. Both palladium atoms are in a square planar environment: the τ_4 parameters are 0.04 for Pd1 and 0.05 for Pd2. The Pd – N and Pd – Cl bond lengths and angles are similar to the values found for other compounds containing PdCl$_2$ groups coordinated by nitrogen-based ligands.

The DMSO solvent of crystallization is positioned between two molecules of **2**, Figure 4b. The C-H hydrogen atom (from the amide end) is involved in a hydrogen bond with the oxygen atom from DMSO, while the sulfur atom is situated on top of two pyrazolyl rings of an adjacent molecule of the complex. As shown in Figure 4b by the blue dotted lines, each DMSO molecule interacts with a hydrogen atom, the C-H···O interaction parameters being 1.952 Å for the C(7)-H(7)···O(2) distance, 2.891 Å for the C(7)···O(2) distance, and 155.26° for the C(7)-H(7)-O(2) angle. The rest of the crystal packing of this compound is based solely on van der Waals forces.

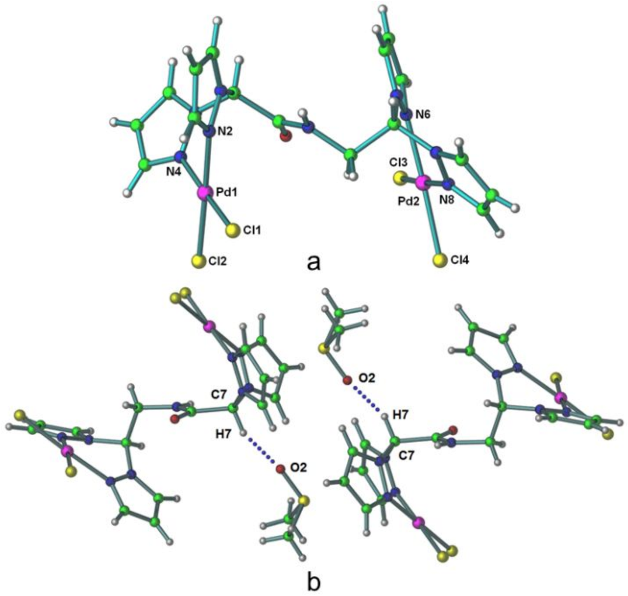

Figure 4. a) The molecular structure of **2**; b) the C-H···O hydrogen bond between a DMSO solvent molecule and the palladium(II) complex; selected bond and angles (Å and °): Pd(1)-N(2)=2.013; Pd(1)-N(4)=2.028; Pd(1)-Cl(1)=2.296; Pd(1)-Cl(2)=2.278; Pd(2)-N(6)=2.030; Pd(2)-N(8)=2.019; Pd(2)-Cl(3)=2.280; Pd(2)-Cl(4)=2.290; N(2)-Pd(1)-N(4)=87.83; N(2)-Pd(1)-Cl(1)=89.56; Cl(1)-Pd(1)-Cl(2)=92.69; Cl(2)-Pd(1)-N(4)=89.91; N(6)-Pd(2)-N(8)=88.96; N(6)-Pd(2)-Cl(3)=90.20; Cl(3)-Pd(2)-Cl(4)=90.13; Cl(4)-Pd(2)-N(8)=90.88; color code: carbon–green, hydrogen–gray, oxygen–red, nitrogen–blue, chlorine–yellow, palladium–purple.

Again, the solid-state structure of **2** is in good agreement with the results obtained from NMR and IR studies. As suggested by the NMR spectrum of the complex and confirmed by its solid-state structure, the amide proton (e) is not involved in hydrogen bonding interactions, and its upfield shift is a consequence of the proton being shielded by the pyrazolyl rings of the ligand. Further, the C-H proton (d) participates in the hydrogen bonding interaction, as suggested by the downfield shift from its original position in the ^{1}H-NMR spectrum of the ligand.

{(L4Pz)[Re(CO)$_3$][Re(CO)$_3$Br]}Br, (3). The reaction of **L4Pz** with two equivalents of Re(CO)$_5$Br in toluene produced a yellow-orange precipitate that was isolated by vacuum filtration. The compound is soluble in acetone, acetonitrile and methanol, and insoluble in halogenated solvents.

The ^{1}H-NMR spectrum of **3** in acetone-d$_6$ (Figure 5a) revealed significant changes in the chemical shifts of the amide (e) and C-H (d) protons, both experiencing a downfield shift of 2.24 ppm and 1.19 ppm, respectively, a clear indication that both protons are involved in strong hydrogen bonding interactions. In addition, one of the two C4 protons of the pyrazolyl ring (b) also experiences a significant downfield shift, ($\Delta\delta$ = 0.53 ppm), while the other (i) is practically not affected by the coordination of the ligand to the Re(I) center ($\Delta\delta$ = 0.06 ppm). These data suggest that the environment around (b) is quite different from the one around (i).

Further, the IR spectrum of **3** recorded in KBr showed that the peak corresponding to the C=O amide stretching vibration shifted to lower wavenumbers (from 1701 cm^{-1} in the free ligand to 1647 cm^{-1} in the complex, $\Delta\tilde{\nu}$ = 54 cm^{-1}, Figure 5b), thus providing a compelling evidence for the coordination of the amide moiety to the Re(I) center. In addition, the characteristic stretching vibrations of the rhenium bound C≡O ligands can be found in the 2043 – 1885 cm^{-1} interval. There are two sharp peaks positioned at 2043 and 2028 cm^{-1}, and a broad band centered at 1912 cm^{-1}. While this data demonstrates that both Re(I) centers have a C$_s$ local symmetry, the presence of two different A' peaks at 2043 and 2028 cm^{-1}, combined with the shift of the C=O amide vibration, suggests different coordination environments around the Re(CO)$_3$ metallic centers: one is coordinated by two pyrazolyl rings and the oxygen atom from the amide group and the other is coordinated by the remaining pyrazolyl groups of **L4Pz**, with the bromide anion completing the coordination sphere around the metal. In a related compound, H$_2$C(pz)$_2$Re(CO)$_3$Cl,[29] one of the A' band was found at 2028 cm^{-1}. In our compound, there is a peak at the same value, which is attributed to the rhenium center having the bromide anion as a ligand. The other peak at 2043 cm^{-1} is attributed to the rhenium center coordinated by the amide group, which is in agreement with the replacement of the bromide anion by the neutral, weaker σ-donor O atom.

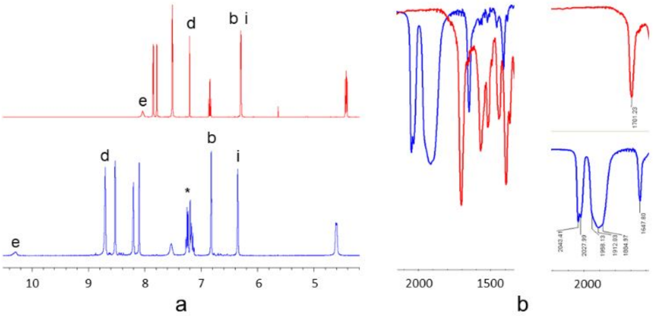

Figure 5. a) ^{1}H-NMR spectra of the ligand (red line – top) and {(**L4Pz**)[Re(CO)$_3$]-[Re(CO)$_3$Br]}Br, (**3**, blue line - bottom); the peak marked with * corresponds to residual toluene solvent molecules; b) IR spectra of the ligand (red line) and **3** (blue line).

The solid-state structure of **3** was determined by single crystal X-ray diffraction. The asymmetric unit contains one {(**L4Pz**)[Re(CO)$_3$][Re(CO)$_3$Br]}$^+$ cation and a bromide anion. The structure of the bimetallic cation is presented in Figure 6 and consists in a **L4Pz** ligand coordinated to two Re(CO)$_3$ centers in a κ^3-μ-κ^2 fashion. The Re(1) atom is coordinated by one bis(pyrazolyl)methane donor set, three CO ligands and one bromide anion, and the Re(2) atom by the other bis(pyrazolyl)methane donor group, three CO molecules and the oxygen atom of the amide moiety. The bond lengths and angles are within the normal range for these types of compounds.

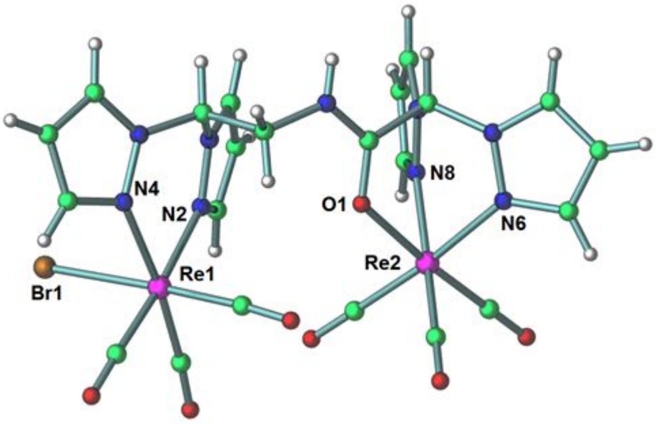

Figure 6. The structure of the {(**L4Pz**)[Re(CO)$_3$][Re(CO)$_3$Br]}$^+$ cation; selected bond and angles (Å and °): Re(1)-Br(1)=2.643; Re(1)-N(4)=2.184; Re(1)-N(2)=2.198; Re(2)-N(8)=2.181; Re(2)-N(6)=2.168; Re(2)-O(1)=2.176; Br(1)-Re(1)-N(4)=83.43; N(4)-Re(1)-N(2)=84.00; O(1)-Re(2)-N(8)=80.86; N(8)-Re(2)-N(6)=82.12; color code: carbon–green, hydrogen–gray, oxygen–red, nitrogen–blue, bromine–brown, rhenium–purple.

These cationic building blocks are assembled into a mono-dimensional tape-like supramolecular architecture (see Figure 7) by two types of non-covalent interactions. The first consist of N-H···Br and C-H···Br hydrogen bonds, as depicted in Figure 8a. The bromide anion is involved in a bifurcated hydrogen bond with the N-H amide proton (e) and the C-H proton (d). The parameters of this interaction are as follows: the N(1)-H(30)···Br(2) and N(1)···Br(2) distances are 2.432 and 3.173 Å, respectively, and the N(1)-H(30)-Br(2) angle is 145.34°. The C(10)-H(10)···Br(2) and C(10)···Br(2) distances are 2.657 and 3.518 Å, respectively, with the corresponding C(10)-H(10)-Br(2) angle of 144.19°. These interactions found in solid state agree with the results obtained from the ^{1}H-NMR study described above: the same protons (e) and (d) experience a large downfield shift of 2.24 ppm and 1.19 ppm, clearly an indication of their involvement in similar hydrogen bonding interactions in solution.

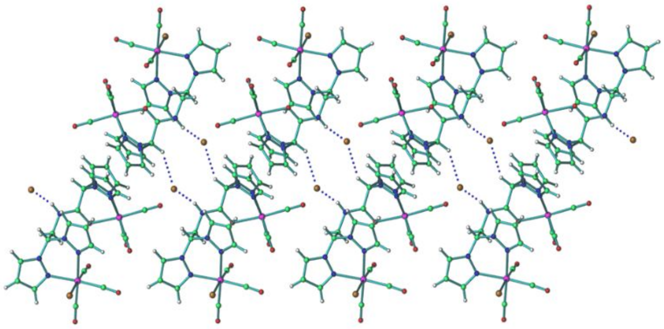

Figure 7. The overall supramolecular structure of {(**L4Pz**)[Re(CO)$_3$][Re(CO)$_3$Br]}Br.

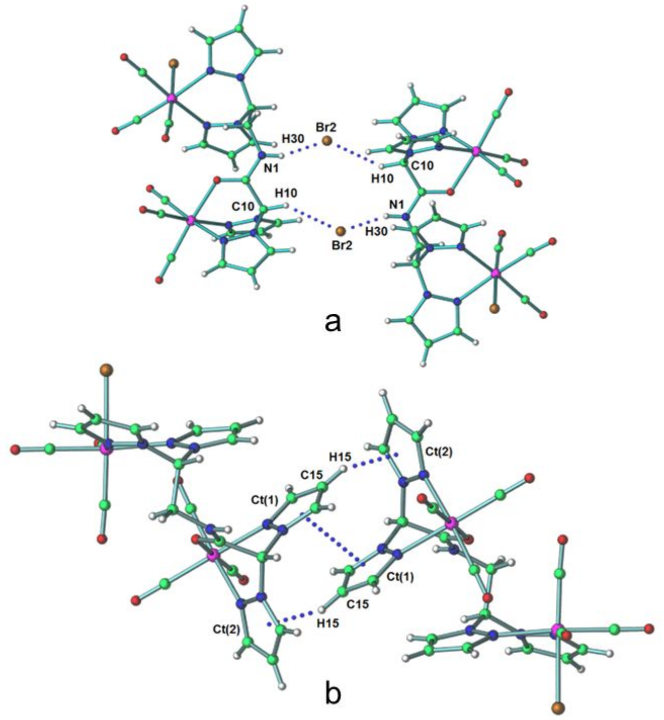

Figure 8. Details of a) hydrogen bonding and b) pyrazolyl embrace in **3**.

The second driving force is a non-covalent interaction termed as “the quadruple pyrazolyl embrace”: a concerted set of π – π stacking and C – H ··· π interactions,[30] shown as blue dotted lines in Figure 8b. Two -C(pz)$_2$ units from the amide side of the ligand are involved in this interaction. For the π – π stacking interaction, the perpendicular distance between the pyrazolyl ring planes is 3.35 Å and the centroid – centroid (Ct1 – Ct1) distance is 3.45 Å, both values significantly below the “cut-off” distance of 3.8 Å for a π···π interaction. The C-H···π interaction has a centroid (Ct2) ··· H distance of 2.65 Å, and a C-H-Ct2 angle of 144.45°. It is worth noting that this pyrazolyl embrace interaction involves the bis(pyrazolyl)methane groups adjacent of the “amide end” of the ligand; this might explain the different chemical shift of the C4 hydrogen atoms of the pyrazolyl rings in the ^{1}H-NMR spectrum of the compound. The C4 proton (b) situated on the pyrazolyl rings involved in the pyrazolyl embrace interaction experiences the largest shift (0.53 ppm), while the corresponding proton (i) situated on the other bis(pyrazolyl)methane group (not involved in any supramolecular interaction) is not affected and shows only a negligible shift of 0.06 ppm.

[(L4Pz)$_2$Fe](BF$_4$)$_2$, (4). The reaction of two equivalents of **L4Pz** with one equivalent of Fe(BF$_4$)$_2$ · 6 H$_2$O in methanol produced a cloudy solution, which, upon concentration, afforded a white precipitate that was isolated by vacuum filtration. Complex **4** is soluble in acetone, acetonitrile, slightly soluble in methanol, and insoluble in halogenated solvents, ether and hexanes. The 2 : 1 ligand to iron(II) ratio in solution was confirmed by Job's method of continuous variations (Figure S5). The same compound (albeit in lower yields) is obtained regardless of the **L4Pz** : iron(II) ratio. The IR spectrum (also shown in Figure S5) substantiates the coordination of the amide moiety to the Fe(II) center: the peak corresponding to the C=O amide stretching vibration shifted to lower wavenumbers (from 1701 cm^{-1} in the free ligand to 1659 cm^{-1} in the complex, $\Delta\tilde{\nu}$ = 42 cm^{-1}).

The ^{1}H-NMR spectrum of this complex is paramagnetically shifted (see Figure S6), with ill-defined, broad peaks, ranging from 47.5 ppm to -45.0 ppm. The magnetic moment of **4** was determined by Evans’ method, and its value of 5.21 μB is consistent with the formation of a high spin, bivalent iron species. This value is similar to those observed for other Fe(II) complexes, such as M[(N(pi^{Cy})$_3$Fe^{II}(H$_2$O)][31] ((N(pi^{Cy})$_3$ = tris(5-cycloiminopyrrol-2-ylmethyl)amine)) or M[(tpaR)Fe^{II}][32] (tpaR = tris(pyrrolyl-R-methyl)amine; M = Na, K; R = mesityl, 2,4,6-triisopropylphenyl, 2,6-difluoro-phenyl, tert-butyl, phenyl), with μ_{eff} values ranging from 5.15 to 5.42 μB.

Colorless crystals of compound **4** were grown from an acetonitrile – diethyl ether system. X-Ray diffraction studies revealed that the asymmetric unit contains one ligand molecule, one Fe(II) cation located on an inversion center, and a tetrafluoroborate counter-ion. The ligand coordinates to the iron center with the “amide end” in a κ^3 binding mode. The octahedral coordination environment around the iron center is depicted in Figure 9, with the nitrogen and oxygen atoms occupying the equatorial and axial positions, respectively. The bond lengths and angles fall within the normal range for this type of complexes, the average of 2.147 Å for the bonds lengths around the metal center agreeing with the high spin state of the iron(II) ion.[33] Once more, the solid-state structure is consistent

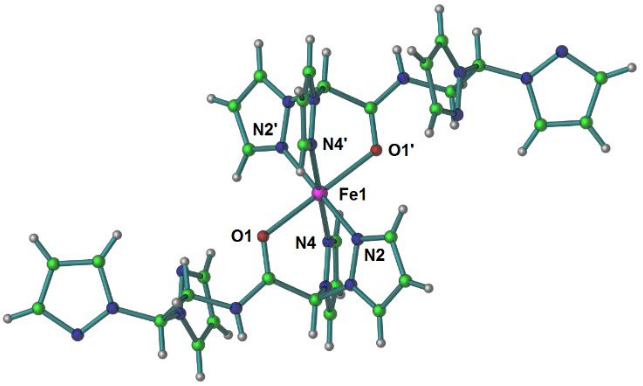

Figure 9. The structure of the [(**L4Pz**)$_2$Fe]$^{2+}$ cation: selected bond and angles (Å and °): Fe(1)-O(1)=2.144; Fe(1)-N(2)=2.154; Fe(1)-N(4)=2.143; O(1)-Fe(1)-N(4)=97.38; N(2)-Fe(1)-N(4)=87.43; O(1)-Fe(1)-N(2)=84.14; color code: carbon–green, hydrogen–gray, oxygen–red, nitrogen–blue, iron–purple.

with the results obtained in solution using Job's method of continuous variations: in both cases a 2 : 1 ligand to metal ratio was found.

The crystal packing of this complex is depicted in Figure 10a and 10b, and consists in mono-dimensional supramolecular chains formed by the pyrazolyl embrace interaction involving the bis(pyrazolyl)methane group coordinated to the iron center, as shown in Figure 10c. For the π – π stacking interaction, the perpendicular distance between the pyrazolyl ring planes is 3.46 Å and the centroid – centroid (Ct1 – Ct1) distance is 3.48 Å, both values significantly below the "cut-off" distance of 3.8 Å for a π···π interaction. The C-H···π interaction has a centroid (Ct2) ··· H distance of 2.67 Å, and a C-H-Ct2 angle of 135.18°. The rest of the crystal packing of **4** is based solely on van der Waals forces.

[(L4Pz)$_2$FeAg](BF$_4$)$_3$, (5). The presence of two uncoordinated bis(pyrazolyl)methane groups in compound **4** prompted us to explore the possibility to prepare mixed metal complexes of the **L4Pz** ligand. The reaction of one equivalent of **4** with one equivalent of AgBF$_4$ in acetonitrile produced, after removal of the volatiles, the mixed metal complex [(**L4Pz**)$_2$FeAg](BF$_4$)$_3$ as a white powder. Compound **5** shows similar properties as its "parent" compound **4**, being soluble in acetone, acetonitrile, slightly soluble in methanol, and insoluble in halogenated solvents, ether and hexanes.

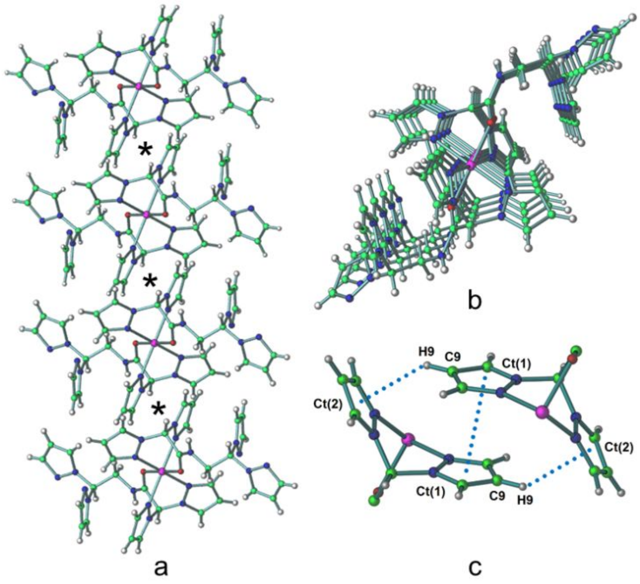

Figure 10. Crystal packing of the [(**L4Pz**)$_2$Fe]$^{2+}$ cation: a) view perpendicular on the chain; b) view along the chain; c) detailed description of pyrazolyl embrace in **4**.

The IR spectrum of **5** is practically identical with the IR spectrum of **4**: the peak corresponding to the C=O amide stretching vibration is positioned at the same wavenumber (1658 cm^{-1}, see Figure S7), suggesting that the coordination of the ligand to the silver center proceeds through the free pyrazolyl rings found in **4**, leaving the amide oxygen coordinated to the Fe(II) ion. Further, the ^{1}H-NMR spectrum of **5** shows only minor differences when compared to the spectrum of complex **4** (Figure S7), with peaks ranging from 48.0 ppm to -48.63 ppm. Further, the magnetic moment of **5** (also determined using the Evans' method) of 4.63 μB, is consistent with a high spin Fe(II) species.

Single crystals of **5** were grown by slow diethyl ether infusion into an acetonitrile solution of the compound and subjected to X-ray diffraction studies. The asymmetric unit of the complex contains two ligand molecules, one Fe(II) cation, one Ag(I) ion and three tetrafluoroborate counter-ions. The structure of the **5**$^{3+}$ cation is depicted in Figure 11 and consists in a Fe-Ag heteronuclear bimetallic macrocycle, formed by a κ^3-μ-κ^2 coordination mode of two **L4Pz** ligands to the iron(II) and silver(I) centers. The iron ion is hexacoordinated by four nitrogen and two oxygen atoms deriving from the "amide end" of the ligand, with similar bond lengths and angles as observed with compound **4**. The average of 2.145 Å for the Fe-N bonds lengths in this compound are practically equal to the one observed in complex **4** (2.147 Å), and consistent with the high spin state of the iron(II) ion. The silver(I) center is positioned in a distorted tetrahedral environment (τ_4 = 0.86), formed by four nitrogen atoms originating from the "amine end" of the ligand.

The crystal packing of this complex (see Figure 12) is based on multiple weak C-H···F hydrogen bonds between the N-H amide protons (e) and both the C-H protons (d – "amide end" and g – "amine end") of the ligand and the fluorine atoms of the BF$_4^-$ counterions.

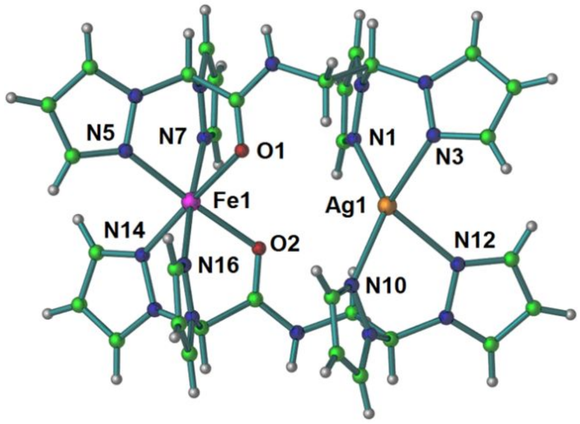

Figure 11. The structure of the [(**L4Pz**)$_2$FeAg]$^{3+}$ (**5**$^{3+}$) cation; selected bond and angles (Å and °): Ag(1)-N(10)=2.259; Ag(1)-N(1)=2.265; Ag(1)-N(3)=2.379; Ag(1)-N(12)=2.398; Fe(1)-N(14)=2.132; Fe(1)-N(5)=2.139; Fe(1)-O(2)=2.140; Fe(1)-N(7)=2.156; Fe(1)-N(16)=2.156; Fe(1)-O(1)=2.173; N1-Ag1-N3=87.48; N10-Ag1-N12=83.79; N10-Ag1-N3=128.76; N1-Ag1-N12=117.54; N5-Fe1-N7=85.06; N14-Fe1-N16=85.18; N14-Fe1-O1=177.47; O2-Fe1-O1=93.91; color code: carbon–green, hydrogen–gray, oxygen–red, nitrogen–blue, iron–purple, silver–orange.

Structural comparison of the metal complexes

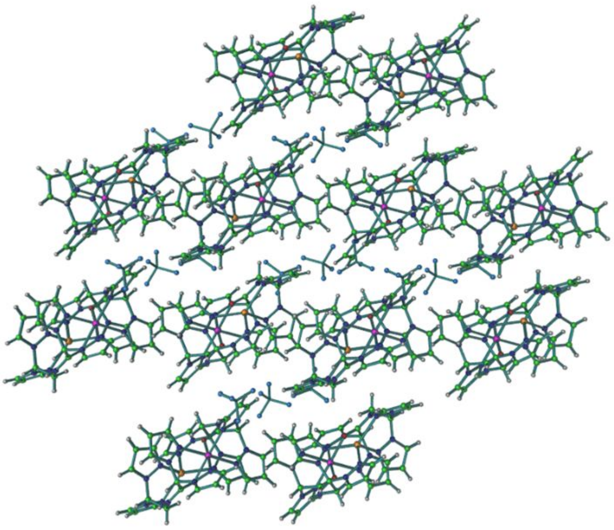

Figure 12. The crystal packing of the [(**L4Pz**)$_2$FeAg](BF4)$_3$ complex.

The structures described above demonstrate the versatility of the **L4Pz** ligand, not only because of its ability to coordinate to metallic centers in either a κ^2-μ-κ^2 or a κ^3-μ-κ^2 fashion, but also because of its predilection to participate in various supra-molecular interactions, such as pyrazolyl embrace and hydrogen bonding. The interplay between these two factors (the ligand-to-metal coordination and the non-covalent interactions) is often responsible for the final (supramolecular) structure of a given compound. The coordination behavior of the “amide end” (κ^2 or κ^3) is determined by the coordination preferences of the metal, as it can be observed by comparing the κ^2 bonding mode found in the structures of complexes **1** and **2** with the κ^3 bonding mode found in complexes **3**, **4**, and **5**.

While **L4Pz** is built on the rigid scaffold of the amide link, the ligand does have some flexibility, thus allowing different orientations of the metallic centers with respect to the amide plane. Figure 13 depicts the structures of the bimetallic complexes **1**, **2**, **3** and **5**, viewed with respect to the (horizontal) plane determined by the O=C-NH atoms of the amide moiety (in the Figure, the oxygen atom is oriented toward the front, and the NH bond points to the back). When the ligand binds to the metallic centers in the κ^2-μ-κ^2 fashion, the -C(pz)$_2$-M group (M = Ag or Pd) can be found either in a *syn* orientation (complex **1**) or in an *anti* configuration (compound **2**). When the ligand acts as a κ^3-μ-κ^2 bridge (that is the amide oxygen is bound to the Re(I) or Fe(II) centers), the metals coordinated by the “amide end” of the ligand are positioned roughly in the same plane as the amide plane (see the structures of complexes **3** and **5**), with the other metal positioned on either side of the plane.

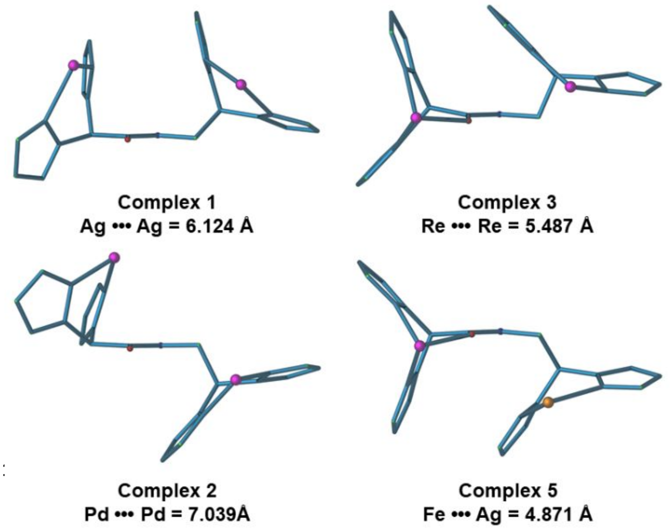

Figure 13. Different orientations of the –C(pz)$_2$-M groups in complexes **1**, **2**, **3**, and **5**; the metal – metal distances are also indicated.

These orientations place the metallic centers at different distances one from another, as can be seen in Figure 13. In the case of the κ^2-μ-κ^2 coordination mode, the metal – metal separations are longer than in the case of the κ^3-μ-κ^2 binding mode. On another hand, comparing complex **1** with complex **2** (both being κ^2-μ-κ^2 bridged by the ligand) we observe that a *syn* orientation provides a metal-metal distance shorter than an *anti* orientation with about 1 Å.

In the presence of silver, the iron-based complex **4** produces a discrete macrocyclic compound, rather than a coordination polymer, as expected based on the opposite orientation of the uncoordinated bis(pyrazolyl)methane groups. To close the macrocycle, one ligand pirouettes around the Fe^{2+} ion from its “original” orientation in the parent compound **4**, thus bringing the four uncoordinated pyrazolyl rings in a suitable position to bind to the Ag$^+$ ion in a tetrahedral fashion. This new orientation of the ligand around the iron center in compound **5** places the two oxygen atoms in a *cis* orientation, in contrast to the parent complex, where the oxygen atoms were found in a *trans* orientation, as pictured in Figure 14a and 14b. Interestingly, the structural features of the ligand scaffold in complexes **4** and **5** are similar. Figure 14c shows a superimposition of the two structures, pictured with respect to the same O=C-NH plane as above. As it can be seen, the most significant difference consists in the different orientation of one uncoordinated pyrazolyl ring in complex **4**.

Conclusions

We have described here the synthesis of a new ditopic ligand, prepared by linking two bis(pyrazolyl)methane donor groups *via* an amide bridge. This ligand (the first member of an entire family of new bis(pyrazolyl)methane ligands) was designed to bind to metallic centers in either a κ^2-μ-κ^2 or a κ^3-μ-κ^2 fashion, depending on the coordination preferences of the central ion.

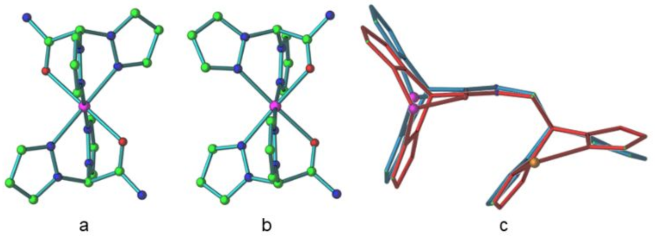

Figure 14. *Trans* vs. *cis* orientation of the oxygen atoms in complex **4** (a) and complex **5** (b); c) overlay of the ligand scaffold in complexes **4** (blue) and **5** (red); color code: carbon–green, oxygen–red, nitrogen–blue, iron–purple.

The reaction of this ligand with silver(I), palladium(II), rhenium(I), and iron(II) starting materials produced compounds having different structural features. Characterization of these compounds revealed that their solution structures are similar to those found in the solid-state. In one case (compound **1**), a coordination polymer was formed, while the others were found to be discrete complexes (compounds **2**-**5**). The ligand coordinates in a κ^2-μ-κ^2 mode in the case of complexes **1** and **2**, and in a κ^3-μ-κ^2 fashion in the case of **3** and **5**. In addition, the presence of acidic hydrogen atoms within the structure of these complexes favored the formation of hydrogen bonds, while the bis(pyrazolyl)methane group triggered association through the pyrazolyl embrace interaction. These intermolecular interactions led to the association of these compounds into various supramolecular architectures.

Moreover, this new ligand provides easy access to hetero-bimetallic complexes, by adapting to the different coordination preferences (*e.g.* octahedral vs. tetrahedral) of different metallic centers. Studies involving this new family of ligands and their metal complexes are underway in our laboratory and will be reported in due course.

Conflicts of interest

There are no conflicts to declare.

Acknowledgements

Acknowledgment is made to the Donors of the American Chemical Society Petroleum Research Fund (grant 56706-UR3) for support of this research. The Single Crystal Diffractometer at EIU was purchased using funds provided by an NSF-MRI grant (CHE-0722547).

Notes and references

1 S. Trofimenko, *J. Am. Chem. Soc.* 1970, **92***,* 5118-5126.

2 (a) A. Otero, J. Fernandez-Baeza, A. Antinolo, J. Tejeda and A. Lara-Sanchez, *Dalton Trans*. 2004, 1499-1510; (b) C. Pettinari and R. Pettinari, *Coord. Chem. Rev*. 2005, **249**, 525-543; (c) C. Pettinari and R. Pettinari, *Coord. Chem. Rev*. 2005, **249**, 663-691; (d) D. L. Reger, *Comments Inorg. Chem*. 1999, **21**, 1-28; (e) H. R. Bigmore, S. C. Lawrence, P. Mountford and C. S. Tredget, *Dalton Trans*. 2005, 635-651; (f) B. R. Manzano, F. A. Jalon, M. C. Carrion and G. Dura, *Eur. J. Inorg. Chem*. 2016, 2272-2295; (g) L M. D. R. S. Martins and A. J. L. Pombeiro, *Coord. Chem. Rev*. 2014, **265**, 74-88; (h) A. Otero, J. Fernandez-Baeza, A. Lara-Sanchez and L. F. Sanchez-Barba, *Coord. Chem. Rev*. 2013, **257**, 1806-1868; (i) G. J. Long, F. Grandjean and D. L. Reger, *Top. Curr. Chem*. 2004, **233**, 91-122; (j) N. Burzlaff, *Adv. Inorg. Chem*. 2008, **60**, 101-165; (k) R. F. Semeniuc and D. L. Reger, *Eur. J. Inorg. Chem*. 2016, 2253-2271.

3 (a) C. Wilfer, P. Liebhaeuser, H. Erdmann, A. Hoffmann and S. Herres-Pawlis, *Eur. J. Inorg. Chem.* 2015, 494-502; (b) A. Hoffmann, U. Floerke and S. Herres-Pawlis, *Eur. J. Inorg. Chem*. 2014, 2296-2306; (c) A. Hoffmann, C. Citek, S. Binder, A. Goos, M. Ruebhausen, O. Troeppner, I. Ivanovic-Burmazovic, E. C. Wasinger, T. D. P. Stack and S. Herres-Pawlis, *Angew. Chem., Int. Ed.* 2013, **52**, 5398-5401; (d) J.-E. Park, S. K. Kang, J. O. Woo and K. Son, *Dalton Trans*. 2015, **44**, 9964-9969.

4 (a) G. Dura, M. C. Carrion, F. A. Jalon, B. R. Manzano, A. M. Rodriguez and K. Mereiter, *Cryst. Growth Des*. 2015, **15**, 3321-3331; (b) G. Dura, M. C. Carrion, F. A. Jalon, A. M. Rodriguez and B. R. Manzano, *Cryst. Growth Des*. 2014, **14**, 3510-3529; (c) G. Dura, M. C. Carrion, F. A. Jalon, A. M. Rodriguez and B. R. Manzano, *Cryst. Growth Des*. 2013, **13**, 3275-3282.

5 (a) M. Strianese, S. Milione, V. Bertolasi, C. Pellecchia and A. Grassi, A. *Inorg. Chem.* 2011, **50**, 900-910; (b) F. Blasberg, J. W. Bats, M. Bolte, H.-W. Lerner and M. Wagner, *Inorg. Chem*. 2010, **49**, 7435-7445; (c) Al. F. R. Kilpatrick, S. V. Kulangara, M. G. Cushion, R. Duchateau and P. Mountford, *Dalton Trans.* 2010, **39**, 3653-3664; (d) M. C. Carrion, F. Sepulveda, F. A. Jalon, B. R. Manzano and A. M. Rodriguez, *Organometallics* 2009, **28**, 3822-3833; (e) A. D. Schofield, M. L. Barros, M. G. Cushion, A. D. Schwarz and P. Mountford, *Dalton Trans.* 2009, 85-96.

6 (a) I. Bassanetti, A. Comotti, P. Sozzani, S. Bracco, G. Calestani, F. Mezzadri and L. Marchio, *J. Am. Chem. Soc.* 2014, **136**, 14883-14895; (b) I. Bassanetti and L. Marchio, *Inorg. Chem*. 2011, **50**, 10786-10797; (c) S. Tardito, I. Bassanetti, C. Bignardi, L. Elviri, M. Tegoni, C. Mucchino, O. Bussolati, R. Franchi-Gazzola and L. Marchio, *J. Am. Chem. Soc.* 2011, **133**, 6235-6242.

7 (a) D. L. Reger, R. F. Semeniuc, J. R. Gardinier, J. O'Neal, B. Reinecke and M. D. Smith, *Inorg. Chem.* **2006***, 45*, 4337-4339; (b) L. Maria, S. Cunha, M. Videira, L. Gano, A. Paulo, I. C. Santos and I. Santos, *Dalton Trans*. 2007, 3010-3019.

8 (a) J. Zhang, A. Li and T. S. A. Hor, *DaltonTrans*. 2009, 9327-9333; (b) D. L. Reger, B. Reinecke, M. D. Smith and R. F. Semeniuc, *Inorg. Chim. Acta* 2009*,* **362**, 4377-4388; (c) S. Pai, M. Hafftlang, G. Atongo, C. Nagel, J. Niesel, S. Botov, H.-G. Schmalz, B. Yard and U. Schatzschneider, *Dalton Trans*. 2014, **43**, 8664-8678.

9 Z. Zhang and D. Cui, *Chem. Eur. J*. 2011, **17**, 11520-11526.

10 (a) Z. Mou, H. Xie, M. Wang, N. Liu, C. Yao, L. Li, J. Liu, S. Li and D. Cui, D. *Organometallics* 2015, **34**, 3944-3949; (b) Z. Mou, B. Liu, M. Wang, H. Xie, P. Li, L. Li, S. Li and D. Cui, *Chem. Commun*. 2014, **50**, 11411-11414; (c) Z. Mou, B. Liu, X. Liu, H. Xie, W. Rong, L. Li, S. Li and D. Cui, *Macromolecules* 2014, **47**, 2233-2241.

11 (a) A. Otero, J. Fernández-Baeza, J. Tejeda, A. Antiñolo, F. Carillo-Hermosilla, E. Díez-Barra, A. Lara-Sánchez, M. Fernández-López, M. Lanfranchi and M. A. Pellinghelli, *J. Chem. Soc. Dalton Trans*. 1999, 3537-3539; (b) A. Otero, J. Fernández-Baeza, J. Tejeda, A. Antiñolo, F. Carillo-Hermosilla, E. Díez-Barra, A. Lara-Sánchez and M. Fernández-López, *J. Chem. Soc. Dalton Trans*. 2000, 2367-2374; (c) N. Burzlaff, I. Hegelmann and B. Weibert, *J. Organomet. Chem.* 2001, **626**, 16-23; (d) A. Beck, B. Weibert and N. Burzlaff, *Eur. J. Inorg. Chem.* 2001, 521-527; (e) F. Marchetti, C. Pettinari, A. Cerquetella, A. Cingolani, R. Pettinari, M. Monari, R. Wanke, M. L. Kuznetsov and A. J. L. Pombeiro, *Inorg. Chem*. 2009, **48**, 6096-6108; (f) G. Tuerkoglu, S. Tampier, F. Strinitz, F. W. Heinemann, E. Huebner and N. Burzlaff, *Organometallics* 2012, **31**, 2166-2174; (g) M. W. Jones, J. E. Baldwin, A. R. Cowley, J. R. Dilworth, A. Karpov, N. Smiljanic, A. L. Thompson and R. M. Adlington, *Dalton Trans*. 2012, **41**, 14068-14086; (h) F. Strinitz, J. Tucher, J. A. Januszewski, A. R. Waterloo, P. Stegner, S. Foertsch, E. Huebner, R. R. Tykwinski and N. Burzlaff, *Organometallics* 2014, **33**, 5129-5144.

12 (a) B. Kozlevcar, T. Pregelj, A. Pevec, N. Kitanovski, J. S. Costa, G. van Albada, P. Gamez and J. Reedijk, *Eur. J. Inorg. Chem*. 2008, 4977-4982; (b) A. Sanchez-Mendez, E. de Jesus, J. C. Flores and P. Gomez-Sal, *Eur. J. Inorg. Chem*. 2010, 141-151.

13 (a) A. Otero, A. Lara-Sanchez, J. A. Castro-Osma, I. Marquez-Segovia, C. Alonso-Moreno, J. Fernandez-Baeza, L. F. Sanchez-Barba and A. M. Rodriguez, *New J. Chem*. 2015, **39**, 7672-7681; (b) S. Bhattacharyya, A. Sarkar, S. K. Dey and A. Mukherjee, *J. Inorg. Biochem*. 2014, **140**, 131-142; (c) S. Bhattacharyya, A. Sarkar, S. K. Dey, G. P. Jose, A. Mukherjee and T. K. Sengupta, *Dalton Trans*. 2013, **42**, 11709-11719; (d) J. A. Castro-Osma, C. Alonso-Moreno, I. Marquez-Segovia, A.

Otero, A. Lara-Sanchez, J. Fernandez-Baeza, A. M. Rodriguez, L. F. Sanchez-Barba and J. C. Garcia-Martinez, *Dalton Trans*. 2013, **42**, 9325-9337; (e) M. Pellei, G. Papini, A. Trasatti, M. Giorgetti, D. Tonelli, M. Minicucci, C. Marzano, V. Gandin, G. Aquilanti, A. Dolmella and C. Santini, *Dalton Trans.* 2011, **40**, 9877-9888; (f) A. Otero, A. Lara-Sanchez, J. Fernandez-Baeza, C. Alonso-Moreno, J. A. Castro-Osma, I. Marquez-Segovia, L. F. Sanchez-Barba, A. M. Rodriguez and J. C. Garcia-Martinez, *Organometallics* 2011, **30**, 1507-1522; (g) A. Otero, J. Fernandez-Baeza, A. Antinolo, J. Tejeda, A. Lara-Sanchez, L. Sanchez-Barba, M. Sanchez-Molina, S. Franco, I. Lopez-Solera and A. M. Rodriguez, *Dalton Trans*. 2006, 4359-4370; (h) A. Otero, J. Fernandez-Baeza, A. Antinolo, J. Tejeda, A. Lara-Sanchez, L. Sanchez-Barba, M. Sanchez-Molina, S. Franco, I. Lopez-Solera and A. M. Rodriguez, *Eur. J. Inorg. Chem*. 2006, 707-710.

14 (a) A. Garces, L. F. Sanchez-Barba, J. Fernandez-Baeza, A. Otero, M. Honrado, A. Lara-Sanchez and A. M. Rodriguez, *Inorg. Chem*. 2013, **52**, 12691-12701; (b) L. F. Sanchez-Barba, A. Garces, J. Fernandez-Baeza, A. Otero, C. Alonso-Moreno, A. Lara-Sanchez and A. M. Rodriguez, *Organometallics* 2011, **30**, 2775-2789; (c) L. F. Sanchez-Barba, C. Alonso-Moreno, A. Garces, M. Fajardo, J. Fernandez-Baeza, A. Otero, A. Lara-Sanchez, A. M. Rodriguez and I. Lopez-Solera, *Dalton Trans*. 2009, 8054-8062.

15 (a) D. L. Reger, A. E. Pascui, M. D. Smith, J. Jezierska and A. Ozarowski, *Inorg. Chem*. 2015, **54**, 1487-1500; (b) D. L. Reger, A. E. Pascui, P. J. Pellechia, M. D. Smith, J. Jezierska and A. Ozarowski, *Inorg. Chem*. 2014, **53**, 4325-4339; (c) D. L. Reger, A. E. Pascui, P. J. Pellechia and M. D. Smith, *Inorg. Chem*. 2013, **52**, 11638-11649; (d) D. L. Reger, A. E. Pascui, M. D. Smith, J. Jezierska and A. Ozarowski, *Inorg. Chem*. 2012, **51**, 11820-11836; (e) D. L. Reger, R. P. Watson, J. R. Gardinier, M. D. Smith and P. J. Pellechia, *Inorg. Chem*. 2006, **45**, 10088-10097.

16 (a) G. Dura, M. C. Carrion, F. A. Jalon, B. R. Manzano and A. M. Rodriguez, *Eur. J. Inorg. Chem*. 2013, 5943-5957; (b) D. L. Reger, A. E. Pascui and M. D. Smith, *Eur. J. Inorg. Chem*. 2012, 4593-4604; (c) J. H. H. Ho, J. Wagler, A. C. Willis and B. A. Messerle, *Dalton Trans*. 2011, **40**, 11031-11042; (d) D. L. Reger, R. P. Watson and M. D. Smith, *Inorg. Chem*. 2006, **45**, 10077-10087.

17 (a) T. J. Morin, S. Wanniarachchi, C. Gwengo, V. Makura, H. M. Tatlock, S. V. Lindeman, B. Bennett, G. J. Long, F. Grandjean and J. R. Gardinier, *Dalton Trans*. 2011, **40**, 8024-8034; (b) T. J. Morin, A. Merkel, S. V. Lindeman and J. R. Gardinier, *Inorg. Chem*. 2010, **49**, 7992-8002.

18 (a) D. L. Reger, J. R. Gardinier, R. F. Semeniuc and M. D. Smith, *J. Chem. Soc., Dalton Trans*., 2003, 1712-1718; (b) D. L. Reger, R. P. Watson, J. R. Gardinier and M. D. Smith, *Inorg. Chem*. 2004, **43**, 6609-6619.

19 (a) D. L. Reger, E. A. Foley, R. F. Semeniuc and M. D. Smith, *Inorg. Chem.* 2007, **46**, 11345-11355; (b) D. L. Reger, E. A. Foley and M. D. Smith, *Inorg. Chem*. 2009, **48**, 936-945; (c) D. L. Reger, E. A. Foley and M. D. Smith, *Inorg. Chem*. 2010, **49**, 234-242; (d) D. L. Reger, E. A. Foley and M. D. Smith, *Inorg. Chem. Comm*. 2010, **13**, 568-572.

20 (a) R. F. Semeniuc, D. L. Reger and M. D. Smith, *Acta Cryst.* 2016, **C72**, 826-831; (b) R. F. Semeniuc, D. L. Reger and M. D. Smith, *Acta Cryst.* 2016, **C72**, 832-837; (c) R. F. Semeniuc, R. R. Baum, J. J. Veach, K. A. Wheeler and P. J. Pellechia, *Inorg. Chim. Acta.* 2013, **400**, 228-238; (d) R. F. Semeniuc, T. J. Reamer and M. D. Smith, *New J. Chem*. 2010, **34**, 439-452; (e) R. F. Semeniuc, T. J. Reamer, J. P. Blitz, K. A. Wheeler and M. D. Smith, *Inorg. Chem.* 2010, **49**, 2624-2629.

21 L. J. Barbour, *J. Supramol. Chem.* 2001, **1**, 189-191.

22 G. M. Sheldrick, *Acta Crystallogr., Sect. A* 2008, **64**, 112-122.

23 (a) T. Kojima, N. Hirasa, D. Noguchi, T. Ishizuka, S. Miyazaki, Y. Shiota, K. Yoshizawa and S. Fukuzumi, *Inorg. Chem*. 2010, **49**, 3737-3745; (b) T. Kojima, K.-I. Hayashi and Y. Matsuda, *Inorg. Chem*. 2004, **43**, 6793-6804; (c) M. Gupta, P. Mathur and R. J. Butcher, *Inorg. Chem*. 2001, **40**, 878-885; (d) F. E. Hahn, H. Schroeder, T. Pape and F. Hupka, *Eur. J. Inorg. Chem*. 2010, 909-917; (e) L. A. Clapp, C. J. Siddons, D. G. VanDerveer, J. H. Reibenspies, S. B. Jones and R. D. Hancock, *Dalton Trans*. 2006, 2001-2007; (f) J. C. M. Rivas, E. Salvagni and S. Parsons, *Dalton Trans*. 2004, 4185-4192; (g) J. C. M. Rivas, E. Salvagni, R. Prabaharan, R. T. Martin de Rosales and S. Parsons, *Dalton Trans*. 2004, 172-177; (h) T. J. Collins, *Acc. Chem. Res.* 1994, **27**, 279-285; (i) R. Gupta, D. C. Lacy, E. L. Bominaar, A. S. Borovik and M. P. Hendrich, *J. Am. Chem. Soc.* 2012, **134**, 9775-9784; (j) D. S. Marlin and P. K. Mascharak, *Chem. Soc. Rev.* 2000, **29**, 69-74.

24 C. A. G. N. Montalbetti and V. Falque, *Tetrahedron* 2005, **61**, 10827-10852.

25 a) M. Ray, A. P. Golombek, M. P. Hendrich, G. P. A. Yap, L. M. Liable-Sands, A. L. Rheingold and A. S. Borovik, *Inorg. Chem.* 1999, **38**, 3110-3115; b) A. Messadi, A. Mohamadou, I. Dechamp-Olivier and L. Dupont, *J. Coord. Chem.* 2012, **65**, 2442-2458; c) S. Meghdadi, M. Amirnasr, S. B. H. Moein Sadat, K. Mereiter and A. Amiri, *Monatsh. Chem.* 2014, **145**, 1583-1594.

26 L. Yang, D. R. Powell and R. P. Houser, *Dalton Trans.* 2007, 955-964.

27 (a) A. Bondi, *J. Phys. Chem.,* 1964, **68***,* 441-451; (b) R. S. Rowland and R. J. Taylor, *J. Phys. Chem.* 1996, **100**, 7384-7391.

28 (a) T. Steiner and G. R. Desiraju, *Chem. Commun*. 1998, 891-892; (b) T. Steiner, B. Lutz, J. van der Maas, A. M. M. Schreurs, J. Kroon and M. Tamm, *Chem.Commun*. 1998, 171-172; (c) T. Steiner, *Angew. Chem. Int. Ed.* 2002, **41**, 48-76.

29 B. Machura, R. Kruszynski, M. Jaworska, P. Lodowski, R. Penczek and J. Kusz, *Polyhedron*, 2008, **27**, 1767-1778.

30 (a) D. L. Reger, J. R. Gardinier, R. F. Semeniuc and M. D. Smith, *Dalton Trans*. 2003, 1712-1718; (b) D. L. Reger, R. F. Semeniuc and M. D. Smith, *Cryst. Growth Des*. 2005, **5**, 1181-1190; (c) D. L. Reger, R. F. Semeniuc and M. D. Smith, *Dalton Trans*. 2008, 2253-2260; (d) D. L. Reger, R. F. Semeniuc, V. Rassolov and M. D. Smith, *Inorg. Chem*. 2004, **43**, 537-554.

31 E. M. Matson, J. A. Bertke and A. R. Fout, *Inorg. Chem.* 2014, **53**, 4450-4458.

32 W. H. Harman, T. D. Harris, D. E. Freedman, H. Fong, A. Chang, J. D. Rhinehart, A. Ozarowski, M. T. Sougrati, F. Grandjean, G. J. Long, J. R. Long and C. J. Chang, *J. Am. Chem. Soc.* 2010, **132**, 18115-18126.

33 O. Kahn and C. J. Martinez, *Science* 1998, **279**, 44-48.

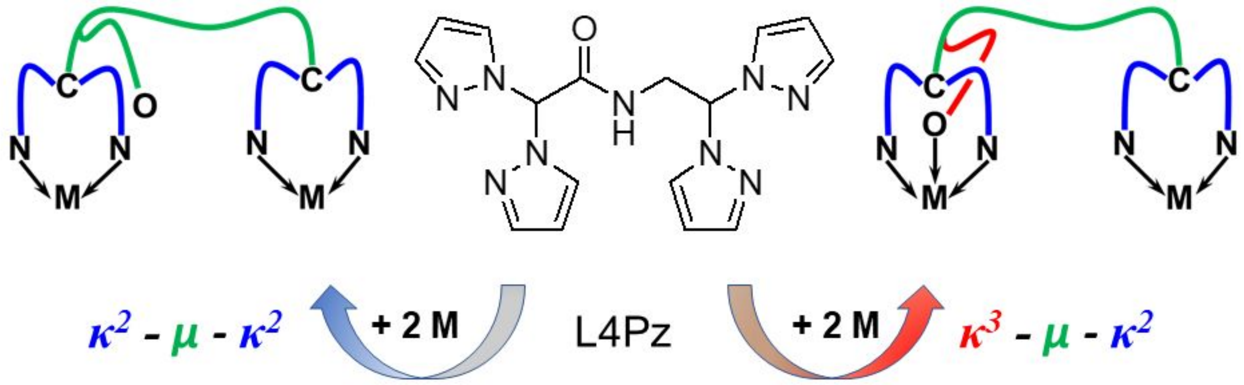

A new ditopic bis(pyrazolyl)methane ligand can coordinate to two metallic centers in either a κ^2-μ-κ^2 or a κ^3-μ-κ^2 mode.